VO2/Si–Al gel nanocomposite thermochromic smart foils: Largely enhanced luminous transmittance and solar modulation

ARTICLE *in* JOURNAL OF COLLOID AND INTERFACE SCIENCE · NOVEMBER 2013

Impact Factor: 3.37 · DOI: 10.1016/j.jcis.2013.11.028 · Source: PubMed

6 AUTHORS, INCLUDING:

Chang Liu
Nanyang Technological University
4 PUBLICATIONS **19** CITATIONS
SEE PROFILE

Yi Long
Nanyang Technological University
27 PUBLICATIONS **175** CITATIONS
SEE PROFILE

Journal of Colloid and Interface Science 427 (2014) 49–53

Contents lists available at ScienceDirect

Journal of Colloid and Interface Science

www.elsevier.com/locate/jcis

VO_2/Si–Al gel nanocomposite thermochromic smart foils: Largely enhanced luminous transmittance and solar modulation

C. Liu [a], X. Cao [a], A. Kamyshny [b], J.Y. Law [a,c], S. Magdassi [b], Y. Long [a,*]

[a] School of Materials Science and Engineering, Nanyang Technological University, 50 Nanyang Avenue, Singapore 639798, Singapore
[b] Institute of Chemistry, Faculty of Science, The Hebrew University, Jerusalem 91904, Israel
[c] Facility for Analysis, Characterization, Testing and Simulation, Nanyang Technological University, 50 Nanyang Avenue, Singapore 639798, Singapore

ARTICLE INFO

Article history:
Available online 20 November 2013

Keywords:
Vanadium dioxide
Nanoparticle
Nanocomposite
Nanothermochromic
Sol–gel
Mechanical bead milling
Smart window

ABSTRACT

VO_2 nanoparticles with a dimension of approximately 20 nm were obtained by simple mechanical bead-milling method, which were well dispersed in transparent silica–alumina (Si–Al) gel matrix to form nanocomposites. The VO_2/Si–Al gel thermochromic nanocomposite foils were fabricated with various VO_2 solid contents and foil thickness. With 10% VO_2 loading and 3 μm foil thickness, high luminous transmittance ($T_{lum(20°C)}$ = 63.7% and $T_{lum(90°C)}$ = 54.4%), and large solar modulation ability (ΔT_{sol} = 12%) can be obtained which surpasses the best reported results (nanoporous films:$T_{lum(20°C)}$ = 43.3%, $T_{lum(90°C)}$ = 39.9% and ΔT_{sol} = 14.1%). This current approach provided a simple and scalable preparation method with the best combined thermochromic performance.

1. Introduction

Vanadium dioxide (VO_2) has been a leading thermochromic material as it exhibits an excellent temperature-responsive behavior at a critical transition temperature (τ_c) of 341 K (68 °C) near room temperature, which makes it an excellent candidate as smart architectural glazing [1]. VO_2 transits from an infrared-transparent semiconductor state at low temperature to an infrared-reflective metallic state at high temperature; nevertheless, it retains visible transmittance [2–4]. However, the low solar energy modulation ability (ΔT_{sol}) and luminous transmittance (T_{lum}) hinder its commercial applications [5–10].

To tackle this issue, Li et al. proposed nanothermochromism, which is defined as integrating VO_2-based nanoparticles into transparent matrix [11]. Based on the computational data, it was claimed that VO_2 nanoparticles dispersed in a dielectric host are more advantageous than VO_2 continuous thin solid films in smart window applications as they offer much higher T_{lum} and enhanced ΔT_{sol}. The crystalline VO_2 nanoparticles produced by hydrothermal and sol–gel methods are used as functional nanofillers in various matrices (e.g.: polyurethane (PU) and polysiloxane) to form nanocomposite foils on various substrates (e.g.: float glass and polyethylene terephthalate (PET)) [12–15]. The T_{lum} and ΔT_{sol} based on nanothermochromism are summarized in Table 1, and are compared with the best performing nanoporous films [16]. None of the current coatings or nanocomposites could satisfy the requirement for a practical architectural window (T_{lum} > 60%) while still maintaining a large solar modulation ability (ΔT_{sol} > 10%) [17,18].

Hereby, we introduce a facile and scalable approach to prepare thermochromic foils with mechanically attrited VO_2 nanoparticles dispersed in a transparent silica–alumina (Si–Al) gel. With the optimization of VO_2 solid content and foil thickness, the foils with high visible transparency and large solar modulation ability can be obtained. This result offers ~15% enhancement of $T_{lum(average)}$ (59.1% vs. 51.4%) and comparable ΔT_{sol} (12.0% vs. 11.7%) as compared with the best reported nanothermochromic foils [13] as highlighted in Table 1.

2. Experimental section

2.1. Preparation of VO_2 nanoparticles

The crystalline VO_2 nanoparticles were prepared by simple bead-milling method. The micro-sized commercial VO_2 powder 23 wt% (originally 99%, Alfa Aesar) was dispersed in an organic solvent, dipropylene glycol methyl ether (DPM), in the presence of a dispersing agent, Disperbyk 180 (4.5 wt%). Subsequently, the obtained dispersion was milled for 4 h in Dyno-Mill Research Lab WAB with the use of zirconia beads at the speed of 4200 rpm, followed by settling in the ambient condition for 2 days. The nano-sized particles with nano-size were suspended in the colloidal solution, which were used for the following experiments.

* Corresponding author. Fax: +65 67911604.
E-mail address: longyi@ntu.edu.sg (Y. Long).

0021-9797/$ - see front matter © 2013 Elsevier Inc. All rights reserved.
http://dx.doi.org/10.1016/j.jcis.2013.11.028

Table 1
Summary of recent studies on VO_2 nanothermochromic composites.

Matrix	Nanofiller		Substrate	$T_{lum(20°C)}$	$T_{lum(90°C)}$	ΔT_{sol}
	Particles	Synthesis method				
Polysiloxane	Tungsten–doped VO_2	Sol–gel	Float glass	~60.0% at 550 nm		~23.2% at 2.5 μm [12]
PU	VO_2@SiO_2 core–shell	Hydrothermal	PET	~55.3%	~54.2%	~7.5%
				~29.2%	~26.3%	~13.6% [15]
Sb:SnO_2 (ATO)/PU	VO_2	Hydrothermal	PET	~53.0%	~49.8%	~11.7% [13]
PU	Fluorine-doped VO_2	Hydrothermal	PET	~48.7%	~45.9%	~10.7% [14]
Ref: Nanoporous thermochromic VO_2 film[a]			Fused silica	~43.3%	~39.9%	~14.1% [16]

[a] The best reported results on thermochromic smart window films.

2.2. Preparation of VO_2/Si–Al gel nanocomposites on float glass

The nano-sized dispersed VO_2 particles were mixed in a Si–Al gel with a series of solid content, 2.5%, 5%, 10%, 12.5% and 15%. The preparation method of Si-Al gel was reported by us previously [19]. The VO_2 nanoparticles and Si–Al gel were mixed using the Vortex Mixer (Thermo Fisher Scientific Inc.) for 1 h to obtain a homogeneous composite gel. Finally, this VO_2/Si–Al gel nanocomposite was casted onto a float glass substrate as shown in Fig. 1.

2.3. Characterization

The morphologies and phase of VO_2/Si–Al gel nanocomposites were determined by X-ray diffraction (XRD) and transmission electron microscopy (TEM). The micrographs and energy spectroscopic images (ESI) were collected using a Carl Zeiss LIBRA®120 in-column energy filter TEM equipped with an integrated OMEGA filter. XRD was performed using a Bruker D8 Advance diffractrometer (Cu Kα, λ = 0.15406 nm) with 40 kV and 30 mA. The particle size and distribution of the VO_2 nanoparticles in DPM dispersion were measured by a Nano S particle size analyzer (Malvern Instruments Co., Ltd., UK). The optical transmittance in the range of 250–2500 nm was measured with a UV–Vis-NIR spectrophotometer (Cary 5000, Agilent Ltd.) equipped with a Linkam PE120 system peltier simple heating and cooling stage.

The integral luminous transmittance (T_{lum}, 380–780 nm) and solar transmittance (T_{sol}, 280–2500 nm) were calculated based on the recorded spectra using the following expression:

$$T_{lum/sol} = \int \varphi_{lum/sol}(\lambda)T(\lambda)d\lambda / \int \varphi_{lum/sol}(\lambda)d\lambda$$

where $T(\lambda)$ is the recorded foil transmittance, φ_{lum} is the standard luminous efficiency function for the photopic vision of human eyes [20], and φ_{sol} is the solar irradiance spectrum for air mass 1.5 (corresponding to the sun standing 37° above the horizon) [21]. ΔT_{sol} is attained from $\Delta T_{sol} = T_{sol(20°C)} - T_{sol(90°C)}$.

3. Results and discussion

3.1. Preparation of crystalline VO_2 nanoparticles

As shown in Fig. 2, after 4 h milling and 2-day sedimentation, only the nanoparticles with an average size of ~329 nm were suspended in the dispersion and they were employed in this study. The inset shows the XRD patterns for the commercially available VO_2 microparticles (before bead milling) and nano-sized VO_2

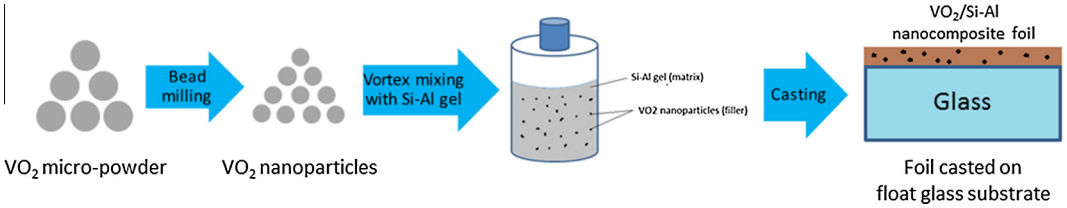

Fig. 1. Preparation procedure of VO_2 nanoparticles and VO_2/Si–Al gel nanocomposite foils on float glass substrates.

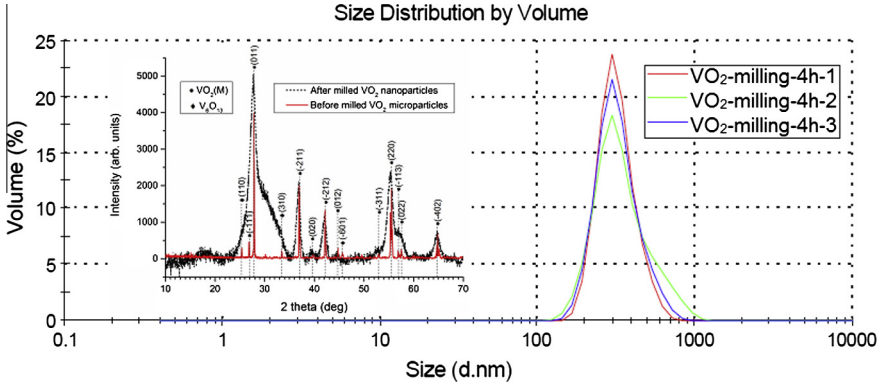

Fig. 2. Particle size and distribution of VO_2 nanoparticles after bead-milling for 4 h; The Inset XRD patterns of the commercial VO_2 microparticles (red solid line) and after-milled VO_2 nanoparticles (black dotted line). (For interpretation of the references to color in this figure legend, the reader is referred to the web version of this article.)

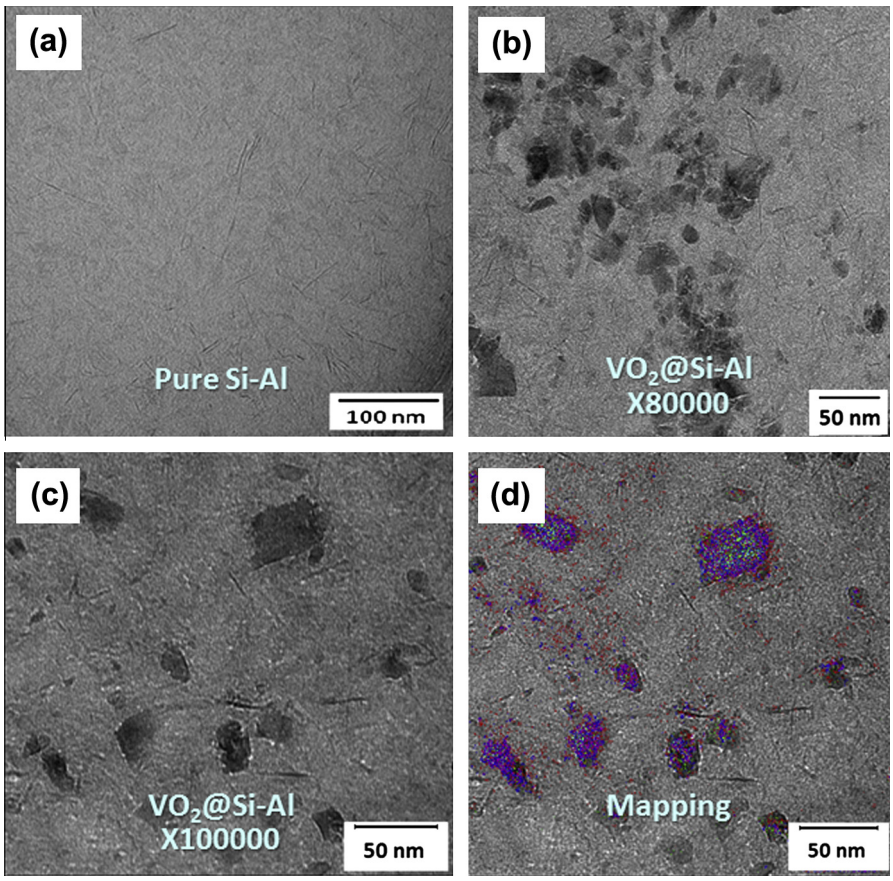

Fig. 3. TEM micrographs of (a) pure Si–Al gel, (b) VO_2/Si–Al gel nanocomposite foil with 10% solid content at a low magnification (×80,000), (c) at a higher magnification (×10,000), (d) TEM ESI mapping image of 3(c) (green:vanadium (V); blue:silicon (Si); red:aluminum (Al)). (For interpretation of the references to color in this figure legend, the reader is referred to the web version of this article.)

particles after bead milling for 4 h. The two XRD patterns were normalized to the respective maximum intensities. The XRD data (Fig. 2 inset) of the commercial VO_2 microparticles show that monoclinic VO_2 (M1, JCPDF No.: 82-661) is the major phase with some minor peaks (solid squares) that are mostly contributed by V_6O_{13} (JCPDF No.: 89-100). After milling, the VO_2 monoclinic phase was maintained in nanoparticles. Meanwhile, the broadening of the full width at half maximum (FWHM) for the main peaks of after-milled sample can be clearly observed, which could be resulted from nanoscale effects. Theoretical calculations based on the Scherrer equation were applied to the (1 1 0) reflection for both before- and after-milled samples and the results indicate that the crystal size of VO_2 particles has been changed from greater than 100 nm to ~10.7 nm after bead milling, which suggests that the bead milling leads to a reduction in VO_2 crystal size without distorting its crystal structure and hence securing the thermochromic properties.

3.2. VO_2/Si–Al gel nanocomposite with different solid contents

Fig. 3(a) displays a TEM image of pure Si–Al gel, which has homogeneous appearance and uniform morphology. Fig. 3b and c shows the morphology and distribution of VO_2 nanoparticles in the Si–Al gel matrix at different magnifications. The milled particles are non-spherical in shape and well dispersed in the matrix with no agglomeration and the particle size is approximately 20 nm. The observed particle size is less than the particle analyzer result (Fig. 2) which may be due to the fact that the agglomerated particles after attrition were de-agglomerated during the Vortex mixing with Si–Al gel and the polyvinylpyrrolidone (PVP) in the gel may help to disperse the VO_2 nanoparticles uniformly in the gel matrix. Fig. 3(d) shows the TEM ESI mapping image of Fig. 3(c). It can be noticed that more Si and Al were migrated onto the surface of VO_2 nanoparticles in contrast to gel phase, forming a shell-like structure which encapsulates the VO_2 nanoparticles. This aggregation of Si and Al may be due to the reason that the VO_2 nanoparticles provide the heterogeneous growth sites for Si and Al favorably depositing on particles to reduce the overall free energy.

Table 2
The thermochromic properties of VO_2/Si–Al gel nanocomposite foils with different solid content ratios of VO_2 nanoparticles.

Solid content of VO_2 (wt%)	T_{lum} (%)		T_{sol} (%)		ΔT_{sol} (%)
	20 °C	90 °C	20 °C	90 °C	
2.5	80.3	81.9	76.7	76.7	−0.01
5.0	69.8	69.2	67.1	61.6	5.5
10.0	59.5	57.1	59.2	51.3	7.9
12.5	55.6	53.4	56.9	50.1	6.8
15.0	56.0	56.3	57.1	55.5	1.6

Table 2 shows the variation in the thermochromic properties of the VO_2/Si–Al gel nanocomposites with different VO_2 solid contents with fixed foil thickness of ~3.3 μm. At a low VO_2 solid content ratio of 2.5%, the composite foil indicated a high T_{lum} but negligible ΔT_{sol}. As VO_2 loading was increased to 10%, the T_{lum} was reduced with increasing ΔT_{sol} and the optimized combination of thermochromic properties (T_{lum}~60% and ΔT_{sol}~8%) can be

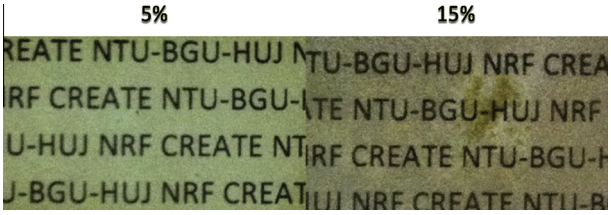

Fig. 4. Photographs of samples with different solid contents of VO_2 nanoparticles at 5% and 15%.

achieved. This could be understood since with increasing VO_2 loading, more thermochromic nanofillers contributed in enhancing ΔT_{sol} while more visible light was scattered and absorbed, leading to reduced $T_{lum.}$ On the other hand, both optical transmittance and solar modulation ability were decreased, when the solid content was greater than 10%. This was due to the fact that when the loading of VO_2 nanoparticles exceeded 10%, the dispersion was no longer transparent and uniform. As shown in Fig. 4, the composite prepared in a low (~5%) solid content produces a clear and flawless morphology, while the high (~15%) solid content sample presented many large particles agglomerates.

3.3. VO_2/Si–Al gel nanocomposites with different foil thicknesses

The UV–Vis-NIR spectra of VO_2/Si-Al gel nanocomposites with different foil thicknesses (1, 1.4, 2, 3μm) with fixed VO_2 solid content of 10% are shown in Fig. 5(a) and the calculated T_{lum} and ΔT_{sol} are shown in Table 3. It can be seen that with increasing thickness, the transmission difference at 2500 nm (ΔT_{sol}@2.5μm) was amplified from 1.67%, 6.24%, 6.35% to 13.83% and ΔT_{sol} was boosted from 0.45% to 12.0% (as shown in Fig. 5b), accompanied by enhanced solar heat shielding ability ($1 - T_{sol(90°C)}$) [13], which efficiently assists to minimize the solar heat as well as the energy demanded for cooling in buildings during the hot summer [11,22].

Table 3
The thermochromic properties of VO_2/Si-Al nanocomposite foils with different foil thicknesses.

Thickness (μm)	T_{lum} (%)		T_{sol} (%)		ΔT_{sol} (%)
	20 °C	90 °C	20 °C	90 °C	
1.0	78.7	79.4	74.9	74.4	0.5
1.4	71.1	71.2	68.1	65.2	2.9
2.0	72.0	69.4	68.8	63.4	5.4
3.0	63.7	54.4	61.9	49.9	12.0

The photographs of foils with 1 μm and 3 μm thickness are shown in Fig. 5c and both foils are flawless and transparent. 3 μm thickness foil provides dark brown color as contrasted to light greenish color in 1μm foil due to less solid content.

It is worth noting that the sample with foil thickness of 3 μm provides large ΔT_{sol} (~12.0%) with combined high integrated averaged T_{lum} (~60%). This result surpasses the best performing nanothermochromic foils on PET substrates [13] as highlighted in Table 1. One of the possible reasons could be due to the differences in the light transmittance of glass and PET substrates as the glass has higher T_{lum} than PET [22]. Compared with nanoporous films [16], with slightly reduced ΔT_{sol} (12% vs. 14.1%), dramatically enhanced averaged T_{lum} (59% vs. 41.6%) can be achieved. This may be due to the uniform dispersion of the nanoparticles in the gel matrix and much decreased particle size (~20 nm) which is well below the wavelength of visible light (refer to Fig. 3).

4. Conclusion

In conclusion, VO_2 nanoparticles with a dimension of approximately 20 nm were successfully obtained by simple mechanical bead-milling method and VO_2/Si–Al nanocomposite foil was formed by mixing the attrited VO_2 with Si–Al gel. This simple and scalable approach produced samples with significantly enhanced T_{lum} (~60%), large ΔT_{sol} (~12%). This combination of both enhanced T_{lum} and ΔT_{sol} exceeds the best reported

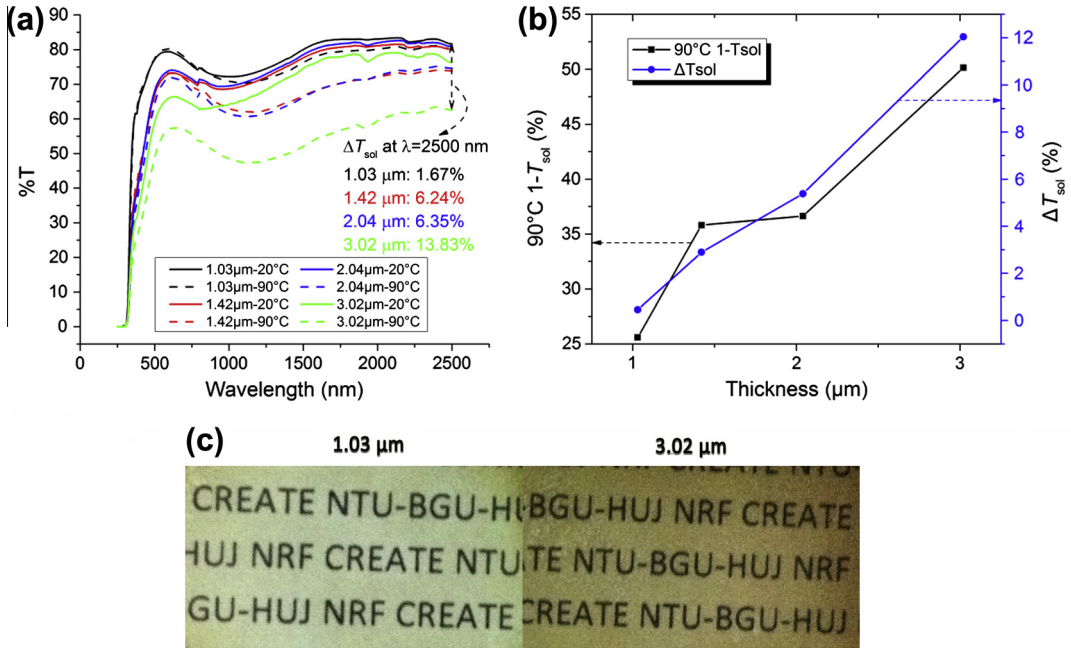

Fig. 5. (a) Transmittance spectra of foils with different thicknesses, (b) $1-T_{sol(90°C)}$ and ΔT_{sol} change with the thickness of VO_2/Si–Al gel nanocomposites (Note: higher $1-T_{sol(90°C)}$ indicating better solar heat shielding ability in summer time), (c) Photographs of samples with different foil thicknesses at 1.03 μm and 3.02 μm.

nanothermochromic samples and nanoporous sample. It is the first result with T_{lum} (~60%) and ΔT_{sol} (>10%) which satisfies the optical qualifications for the potential commercial applications in smart windows.

Acknowledgments

This research was supported by the Singapore National Research Foundation under CREATE program: Nanomaterials for Energy and Water Management. The electron microscopy and XRD work were performed at the Facility for Analysis, Characterization, Testing and Simulation (FACTS) in Nanyang Technological University, Singapore.

References

[1] M. Saeli, C. Piccirillo, I.P. Parkin, R. Binions, I. Ridley, Energy Build. 42 (2010) 1666.
[2] P.V. Kamat, J. Phys. Chem. Lett. 2 (2011) 839.
[3] J. Nag, R.F. Haglund, J. Phys.-Condens. Mater. 20 (2008) 264016.
[4] N. Wang, Y. Huang, S. Magdassi, D. Mandler, H. Liu, Y. Long, RSC Adv. 3 (2013) 7124.
[5] M. Zhou, J. Bao, M. Tao, R. Zhu, Y. Lin, X. Zhang, Y. Xie, Chem. Commun. 49 (2013) 6021.
[6] N. Wang, S. Magdassi, D. Mandler, Y. Long, Thin Solid Films 534 (2013) 594.
[7] Y.F. Gao, H.J. Luo, Z.T. Zhang, L.T. Kang, Z. Chen, J. Du, M. Kanehira, C.X. Cao, Nano Energy 1 (2012) 221.
[8] Z.T. Zhang, Y.F. Gao, Z. Chen, J. Du, C.X. Cao, L.T. Kang, H.J. Luo, Langmuir 26 (2010) 10738.
[9] S.Y. Li, G.A. Niklasson, C.G. Granqvist, J. Appl. Phys. 109 (2011) 113515.
[10] N.R. Mlyuka, G.A. Niklasson, C.G. Granqvist, Appl. Phys. Lett. 95 (2009) 171909.
[11] S.Y. Li, G.A. Niklasson, C.G. Granqvist, J. Appl. Phys. 108 (2010) 063525.
[12] Y.F. Lu, S.X. Zhou, G.X. Gu, L.M. Wu, Thin Solid Films 534 (2013) 231.
[13] Y.F. Gao, S.B. Wang, L.T. Kang, Z. Chen, J. Du, X.L. Liu, H.J. Luo, M. Kanehira, Energy Environ. Sci. 5 (2012) 8234.
[14] L. Dai, S. Chen, J.J. Liu, Y.F. Gao, J.D. Zhou, Z. Chen, C.X. Cao, H.J. Luo, M. Kanehira, Phys. Chem. Chem. Phys. 15 (2013) 11723.
[15] Y.F. Gao, S.B. Wang, H.J. Luo, L. Dai, C.X. Cao, Y.L. Liu, Z. Chen, M. Kanehira, Energy Environ. Sci. 5 (2012) 6104.
[16] L.T. Kang, Y.F. Gao, H.J. Luo, Z. Chen, J. Du, Z.T. Zhang, ACS Appl. Mater. Int. 3 (2011) 135.
[17] M.A. Sobhan, R.T. Kivaisi, B. Stjerna, C.G. Granqvist, Sol. Energy Mater. Sol. Cells 44 (1996) 451.
[18] C.S. Blackman, C. Piccirillo, R. Binions, I.P. Parkin, Thin Solid Films 517 (2009) 4565.
[19] C. Liu, N. Wang, Y. Long, Appl. Surf. Sci. 283 (2013) 222.
[20] G. Wyszecki, W.S. Stiles, Color Science: Concepts and Methods, Quantitative Data and Formulae, second ed., Wiley, New York, 2000.
[21] ASTM G173-03. Standard Tables of Reference Solar Spectral Irradiance. Direct Normal and Hemispherical on a 37° Tilted Surface, Annual Book of ASTM Standards, American Society of Testing and Materials, Philadelphia, PA, 2003.
[22] S. Elmas, Ş. Korkmaz, S. Pat, Appl. Surf. Sci. 276 (2013) 641.